MRS Advances © 2016 Materials Research Society
DOI: 10.1557/adv.2016.375

# Surface-Functionalizing Metal, Metal Oxide and Semiconductor Nanocrystals with a Multi-coordinating Polymer Platform

Wentao Wang, Xin Ji, Anshika Kapur, and Hedi Mattoussi
Department of Chemistry and Biochemistry, Florida State University, Tallahassee, FL 32306

## ABSTRACT

We introduce a new set of multifunctional metal-coordinating polymers as ligands for the surface functionalization of three different inorganic nanocrystals: luminescent quantum dots (QDs), magnetic iron oxide nanocrystals and metal gold nanoparticles. The ligand design relies on the introduction of a large but controllable number of anchoring groups, hydrophilic moieties and reactive functionalities all in the same polymer chain, via a one-step nucleophilic addition reaction. Nanocrystals capped with these polymer ligands exhibit long-term stability over a broad range of biological conditions. Furthermore, when zwitterion groups are introduced as hydrophilic blocks, this yields a compact ligand coating that allows conjugation of biomolecules to the nanocrystals via metal-histidine self-assembly. The resulting hydrophilic nanocrystals have been used to develop a few specific sensing platforms targeting soluble iron ions and cysteine.

## INTRODUCTION

Nanomaterials made of semiconductors, metals and metal oxides possess unique optical and physical properties which can be tuned via size and/or composition.[1-3] For instance, semiconductor nanocrystals such as those made of ZnS-overcoated CdSe QDs exhibit narrow tunable emission throughout the visible spectrum, combined with high quantum yield and extended photo-stability.[4-7] An effective integration of these inorganic nanomaterials into biological systems has the potential to provide novel hybrid platforms that can advance our understandings of several challenging problems in biology.[8, 9] This, however, requires access to hydrophilic nanoparticles that are colloidally stable and present surface-reactive groups.[10, 11] Cap exchange with bifunctional coordinating ligands has been used by several groups to promote the dispersion of various inorganic nanocrystals in buffer media. This strategy relies on the competitive removal of the native hydrophobic capping molecules and their replacement with hydrophilic metal-coordinating ligands. The strength of the ligand coordination onto the nanocrystal surface along with a strong affinity of the hydrophilic modules to buffer media ultimately controls the long-term colloidal stability of the nanocrystals in biological environments. Here, we introduce a new set of multi-coordinating and multifunctional polymer ligands that provide nanocrystals excellent long-term colloidal stability and controllable surface reactive groups that can be used for bioconjugation.

## EXPERIMENTAL SECTION

*Synthesis*. The amphiphilic polymers used for the functionalization of QDs, iron oxide nanocrystals and gold nanoparticles were all based on the nucleophilic addition reaction starting from the poly(isobutylene-*alt*-maleic anhydride), PIMA, precursor and synthesized following previously reported protocols; these include lipoic acid (LA)- and polyethylene glycol (PEG)-

modified polymer (LA-PIMA-PEG), LA/histamine- and PEG-modified polymer (LA/His-PIMA-PEG), dopamine- and PEG-modified polymer (Dopa-PIMA-PEG) and histamine and zwitterion-modified polymer (His-PIMA-ZW).[12-14]. Core-shell CdSe-ZnS quantum dots were synthesized following reported chemical rationales based on hot injection techniques.[5-7] Cap exchange of QDs with LA-containing polymer ligands was carried out under borohydride-free conditions using a mild photoligation strategy, as reported in the previous report.[13] Water solubilization of QDs with His-PIMA-ZW was carried out via ligand exchange using a two-phase mixture of chloroform and dimethyl sulfoxide.[14] Gold and iron oxide NPs were prepared as reported in previous protocols.[12, 15] Surface modification of oleylamine-capped AuNPs with LA-PIMA-PEG and oleic acid-capped iron oxide with Dopa-PIMA-PEG were carried out using a one-phase ligand exchange in chloroform and tetrahydrofuran, respectively.[12, 15]

*Assembly QD-protein conjugates*. Genetically engineered fluorescent protein, mCherry, was self-assembled on the QD with varying conjugate valence. Aliquots of a stock QD dispersion (22.2 μL, 3.6 μM) were loaded into Eppendorf tubes and the volume in each tube was adjusted by adding different amount of phosphate buffer (pH 8.0, 40 mM) to bring the total volume of the dispersion to100 μL. The desired amounts of mCherry solutions were loaded into separate tubes, followed by the addition of phosphate buffer bringing the total volume to 300 μL. The mCherry solutions were gently mixed with the QD dispersions and the resulting mixtures were incubated at 4 ˚C for 30 min to allow for QD-protein self-assembly. The ratio of mCherry-to-QD (i.e., valence) probed in this study was varied from 0:1 to 12:1.

*QD-dopamine conjugates as specific sensors*. The QD-dopamine conjugates were prepared following the steps reported in previous work.[14] For cysteine sensing, aliquots of the QD-dopamine conjugates (40 μL) were dispersed in phosphate buffer (pH 10, 10 mM), then the desired volumes of cysteine stock solution (0.1 mM) were added. The final volume of dispersions was adjusted to 1 mL by adding the required amounts of pH 10 buffer. The mixtures were incubated for different time periods and the PL spectra were recorded after each period. For iron ion sensing, conjugates with given dopamine valence were prepared as described in reference 14, starting with dopamine-ITC. Aliquots of the QD-dopamine dispersions (50 μL) were diluted in DI water and mixed with the desired volume of Fe solution (from a stock solution of Fe ion (2 mM) freshly prepared by dissolving $FeCl_3 \bullet 6H_2O$ in DI water). The final total volume of the mixture was 1.5 mL. The concentration of QD-dopamine was fixed at ~ 26.7 nM, while that of Fe ions was varied from 0 to 20 μM.

## RESULTS AND DISCUSSION

### Ligand design

The polymer ligands designed in this work relied on the use of the one-step nucleophilic addition reaction of several distinct amine-containing moieties with the same PIMA precursor.[12, 13, 15] Each resulting modular ligand presents multiple anchoring groups for metal-coordination on the nanocrystal surface, hydrophilic blocks (based on the PEG or zwitterion motif) for water solubilization, along with reactive groups for further bioconjugation. The anchoring groups have been chosen for optimal coordination on each set of nanocrystals. For example, catechol groups have been shown to exhibit strong affinity to iron oxide nanoparticles, while both thiol and imidazole groups have been shown to exhibit strong coordination on ZnS-overcoated (Zn-rich surface) QDs. In addition, Au-to-thiol interaction has been described in serval instances as covalent binding, given the strong affinity reported for this pair. Using this synthetic scheme and

the coordination chemistry rationales, we have prepared dopamine-modified polymer, Dopa-PIMA-PEG, thiol-modified polymer, LA-PIMA-PEG, imidazole- and LA-modified polymer, namely LA/His-PIMA-PEG and His-PIMA-ZW, which were adapted for the surface functionalization of iron oxide nanocrystals, gold nanoparticles and QDs, respectively (see Figure 1). Replacing the PEG chains with the zwitterion motif produces nanocrystals that are very compact in size with thin hydrophilic coating; this strategy yields QDs that can readily self-assemble with full-sized polyhistidine-tagged proteins (see below).

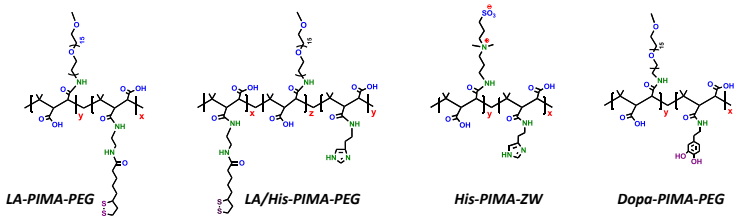


**Figure 1**. Representative ligands used for surface-functionalization of gold nanoparticles, QDs and iron oxide nanocrystals.

## Characterization of the hydrophilic nanocrystals

Surface functionalization of oleylamine-AuNPs and oleic acid-IONPs with the polymer were carried out using one-phase ligand exchange in organic solvents.[12, 15] Ligand exchange of phosphine and phosphine oxide-capped QDs with LA/His-PIMA-PEG was performed using a mild photoligation strategy under sodium borohydride-free conditions, a process facilitated by the photochemical transformation of the dithiolane groups under UV irradiation.[13] This method not only eliminates the tedious preparation and purification of the ligand, but also preserves the integrity of sensitive functionalities, such as azide and aldehyde; the latter are usually altered in the presence of strong reducing agents. For zwitterionic ligand, to circumvent the limited solubility of zwitterion groups in common used organic solvents, the ligands were first dissolved in DMSO then mixed with the hydrophobic QDs dispersed in chloroform.[14]

After ligand exchange and purification, the hydrophilic nanocrystals were characterized using optical spectroscopy or dynamic light scattering (DLS). Figure 2 (A-C) shows the absorption and/or emission spectra for ~10-nm AuNPs, green-emitting QDs (with peak emission at 537 nm and at 556 nm) before and after ligand exchange with LA-PIMA-PEG, LA/His-PIMA-PEG and His-PIMA-ZW, respectively. The spectra of the hydrophilic nanocrystals exhibit essentially identical features to those collected from the native hydrophobic materials, indicating that the integrity of the various nanocrystals following phase transfer was fully maintained. The TEM image in Figure 2D shows that after ligand exchange the IONPs exhibit uniform cores with no sign of etching or aggregation. The DLS data indicates that the hydrophilic nanoparticles have narrow size distribution with low polydispersity index values (PDI $\leq$ 0.1).

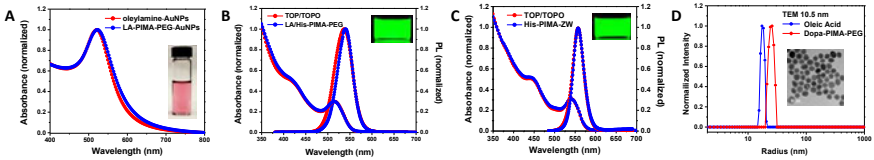


**Figure 2**. (A-C) Optical characterization of gold nanoparticles and QDs before and after ligand exchange. Insets show the white-light image for hydrophilic AuNPs and fluorescence images under UV illumination for QDs. (D) Histograms showing the distribution of the intensity vs. hydrodynamic radius measured (from DLS) for the iron oxide nanoparticles capped with oleic acid and with Dopa-PIMA-PEG in water. The inset shows the TEM image for 10.6 nm iron oxide nanoparticles capped with Dopa-PIMA-PEG.

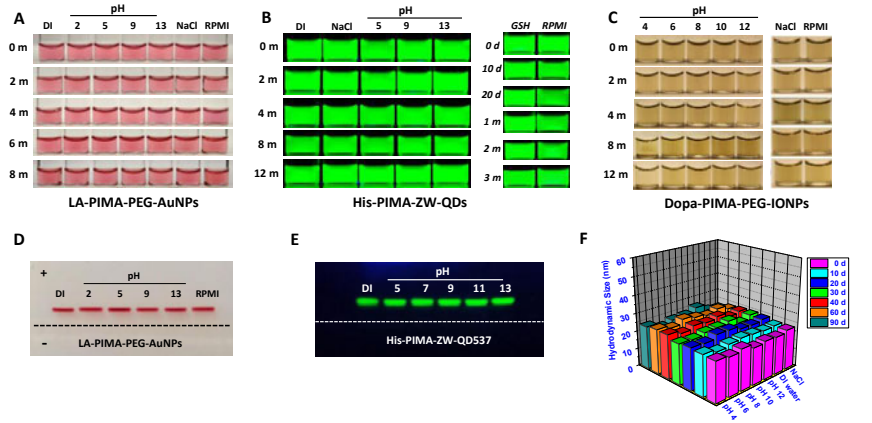


**Figure 3**. (A-C) Colloidal stability tests applied to different polymer-coated nanocrystals (AuNPs, QDs and IONPs) dispersed in DI water, in NaCl solution (1 M), in different pH buffers, in the presence of 10 mM glutathione (GSH, in the case of QDs) and when mixed with growth media (RPMI-1640). Vials are imaged after different storage time (from 0 to 12 months, as indicated) (D and E) Agarose gel electrophoresis images of AuNPs ligated with LA-PIMA-PEG and QDs ligated with His-PIMA-ZW at different pH. The dashed line indicates the location of the loading wells. (F) Time-progression of the apparent hydrodynamic radius measured from Dopa-PIMA-PEG-IONPs in different pH buffers, in DI water and in 1 M NaCl solution.

## Colloidal stability tests

The colloidal stability of aqueous nanocrystals were evaluated under several biologically relevant conditions, including pH changes, dispersion in high ionic strength buffers, in growth media, and in the presence of endogenous thiols, namely glutathione (in the case of QDs). Figure 3 shows white-light images of dispersions of LA-PIMA-PEG-AuNPs, Dopa-PIMA-PEG-IONPs,

as well as the fluorescence images of a set of green-emitting QD dispersions in buffers at different pHs, in 1 M NaCl, and when mixed with growth media (100% RPMI-1640) after several months of storage. The dispersions stayed stable and aggregate-free. In particular, the dispersions of QDs stayed stable for at least 12 months, with no sign of aggregation or loss of fluorescence. Additionally, gel electrophoresis measurements applied to hydrophilic gold nanoparticles and QDs further confirmed the homogenous distribution in size and surface charge (Figure 3 D and E). Dynamic light scattering measurements applied to iron oxide nanoparticles capped with Dopa-PIMA-PEG showed that the hydrodynamic radii of all tested conditions essentially stayed constant after several months of storage (Figure 3F).

## QD-mCherry conjugates: FRET analysis

Self-assembly of the fluorescent mCherry protein appended with a $His_6$-tag onto His-PIMA-ZW-QDs was verified by evaluating the fluorescence resonance energy transfer (FRET) interactions between the QDs and mCherry fluorophores. Figure 4B shows the absorption spectra of QD-mCherry-$His_6$ at a protein-to-QD molar ratio ranging from 0:1 to 12:1. The progressive increase in the absorption peak at ~586 nm is due to mCherry contribution. The corresponding composite emission spectra, collected using excitation at 400 nm, are shown in Figure 4C. Spectra show a progressive loss in QD emission accompanied with a gradual increase in mCherry emission, with the two features tracking the protein-to-QD valence. Since the fluorescence due to direct excitation of the mCherry is negligible, as $\lambda_{ex}$ falls within the protein absorption valley (see profile corresponding to 12:0 in Figure 4C), the fluorescence contribution of the mCherry in the composite spectra is attributed to FRET sensitization of the protein. Using the expression of FRET efficiency for the above conjugate configuration, $E = nR_0^6 / (nR_0^6 + r^6)$ ($R_0$ and $r$ being the Förster radius and QD-to-mCherry center-to-center separation distance, respectively), we extract an experimental estimate for $r$ of ~60 Å.

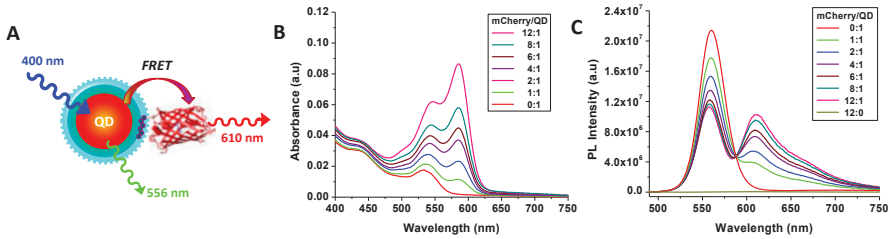


**Figure 4**. (A) Schematic representation of the bioconjugation between His-PIMA-ZW-QDs and proteins driven by polyhistidine coordination. (B, C) Evolution of absorption and emission spectra of QD-mCherry-$His_6$ conjugates when the protein-to-QD ratio (valence) was varied between 0:1 and 12:1.

## QD-dopamine sensing platform

We utilized QD-dopamine conjugates as sensors for probing the interactions of dopamine with iron ions and the amino acid cysteine. For this, we first conjugated dopamine-isothiocyanate (dopamine-ITC) to the hydrophilic QDs capped with amine-functionalized His-PIMA-ZW ligands, to promote covalent attachment via isothiourea bond.[16] This produces sensing platforms

where the fluorescence emission can be modulated by charge transfer (CT) interactions between the central QD and proximal dopamine complexes.[16-18] Figure 5 shows a schematic representation of the proposed modulation of the QD PL via two pathways: (1) Interactions of QD-dopamine with Fe ions in DI water, where Fe-catalyzed oxidation of dopamine increases the concentration of quinone, thus enhancing electron transfer interactions from QDs. This results in pronounced PL loss that directly traces the concentration of added Fe ions. Figure 5B shows the PL spectra collected from dispersions of QD-dopamine conjugates mixed with varying concentrations of Fe ions ranging from 0 µM to 20 µM. Data show that within the range of Fe ion concentration tested the measured PL decrease was linear. (2) Interactions of QD-dopamine conjugates dispersed in pH 10 buffer with cysteine. Here, the thiol group of cysteine reacts with the quinone (dominant at pH 10) to form 5-*S*-cysteinyl-dopamine. This reaction produces a QD PL recovery, due to a reduction in the charge transfer interactions with the QDs, as the concentration of quinone in the medium is decreased. Figure 5C shows the QD PL changes with the reaction time when QD-dopamine conjugates were mixed with 8 µM of cysteine. The QD PL exhibited a progressive increase with time until saturation. Moreover, the normalized PL intensities at saturation were concentration-dependent. These results indicate that transformation from quinone to 5-*S*-cysteinyl-dopamine was faster in the presence of higher concentrations of cysteine (faster reaction kinetics).

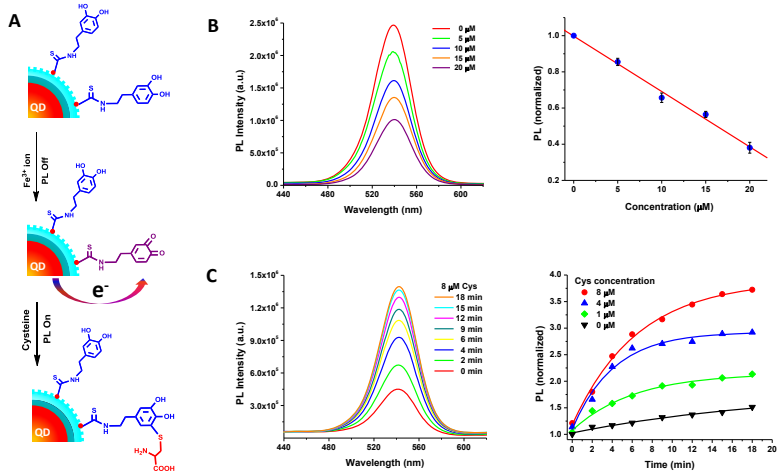


**Figure 5**. (A) Schematic representation of the changes in the charge transfer interactions between QDs and proximal dopamine as a function of introduced iron ions or added cysteine; the QD concentration is fixed. (B) The PL spectra of QD-dopamine conjugates in the presence of different concentrations of Fe from 0 to 20 µM, together with the integrated PL normalized with respect to the value at 0 µM Fe. (C) Time progression of the PL spectra of QD-dopamine conjugates (initially dispersed in pH 10) mixed with 8 µM cysteine. Also shown are plots of the integrated PL progression with time for different concentrations of added cysteine. The PL is normalized with respect to the initial value at 0 min (without cysteine).

## CONCLUSIONS

We have developed a new set of metal-coordinating polymers suited for the surface-functionalization of luminescent QDs, metallic and magnetic nanocrystals alike. The ligand design exploits the highly efficient nucleophilic addition reaction between maleic anhydride and distinct functionalities, namely anchoring groups, hydrophilic moieties, and reactive groups. Ligation with these polymers has yielded hydrophilic nanocrystals that exhibit excellent colloidal stability over a broad range of biological conditions. When zwitterion motifs are used as hydrophilic blocks, this has yielded nanocrystals with small hydrodynamic radius, allowing conjugation of the QDs with polyhistidine-tagged full size proteins. Finally, we have shown that coupling of dopamine to the QDs provides fluorescent platforms that can sense changes in the presence of Fe ions and interactions with cysteine in solution.

## REFERENCES


1. C. B. Murray, C. R. Kagan and M. G. Bawendi, *Annu. Rev. Mater. Sci*. **30**, 545-610 (2000).
2. P. K. Jain, X. H. Huang, I. H. El-Sayed and M. A. El-Sayed, *Acc. Chem. Res*. **41**, 1578-1586 (2008).
3. J. Cheon and J. H. Lee, *Acc. Chem. Res.***41**, 1630-1640 (2008).
4. D. V. Talapin, A. L. Rogach, A. Kornowski, M. Haase and H. Weller, *Nano Lett*. **1**, 207-211(2001).
5. C. B. Murray, D. J. Norris and M. G. Bawendi, *J. Am. Chem. Soc*. **115**, 8706-8715 (1993).
6. Z. A. Peng and X. G. Peng, *J. Am. Chem. Soc*. **123**, 183-184 (2001).
7. B. O. Dabbousi, J. RodriguezViejo, F. V. Mikulec, J. R. Heine, H. Mattoussi, R. Ober, K. F. Jensen and M. G. Bawendi, *J. Phys. Chem. B* **101**, 9463-9475 (1997).
8. K. E. Sapsford, W. R. Algar, L. Berti, K. B. Gemmill, B. J. Casey, E. Oh, M. H. Stewart and I. L. Medintz, *Chem. Rev*. **113**, 1904-2074 (2013).
9. P. D. Howes, R. Chandrawati and M. M. Stevens, *Science* **346**, 1247390 (2014).
10. H. Mattoussi, G. Palui and H. B. Na, *Adv. Drug Deliver. Rev*. **64**, 138-166 (2012).
11. G. Palui, F. Aldeek, W. T. Wang and H. Mattoussi, *Chem. Soc. Rev*. **44**, 193-227 (2015).
12. W. Wang, X. Ji, H. B. Na, M. Safi, A. Smith, G. Palui, J. M. Perez and H. Mattoussi, *Langmuir* **30**, 6197-6208 (2014).
13. W. Wang, A. Kapur, X. Ji, M. Safi, G. Palui, V. Palomo, P. E. Dawson and H. Mattoussi, *J. Am. Chem. Soc*. **137**, 5438-5451 (2015).
14. W. Wang, X. Ji, A. Kapur, C. Zhang and H. Mattoussi, *J. Am. Chem. Soc.* **137**, 14158-14172 ( 2015).
15. W. Wang, F. Aldeek, X. Ji, B. Zeng and H. Mattoussi, *Faraday Discuss.* **175**, 137-151 (2014).
16. X. Ji, G. Palui, T. Avellini, H. B. Na, C. Y. Yi, K. L. Knappenberger and H. Mattoussi, *J. Am. Chem. Soc*. **134**, 6006-6017 (2012).
17. X. Ji, N. S. Makarov, W. T. Wang, G. Palui, I. Robel and H. Mattoussi, *J. Phys. Chem. C*. **119**, 3388-3399 (2015).
18. X. Ji, W. Wang and H. Mattoussi, *Phys. Chem. Chem. Phys.* **17**, 10108-10117 (2015).